Int J Clin Exp Med 2015;8(3):4697-4702
www.ijcem.com /ISSN:1940-5901/IJCEM0004892

Case Report

Intraoperative high-field magnetic resonance imaging combined with neuronavigation-guided resection of intracranial mesenchymal chondrosarcoma in Broca's area: a rare case report and literature review

Jing Yan[1], Jingliang Cheng[1], Hongwei Li[2], Xianzhi Liu[2], Yuan Zheng[3], Chaoyan Wang[1], Wenzheng Luo[2], Yunfei Nie[3], Zhengwei Li[3], Beibei Pang[3], Bo Yang[2]

Departments of [1]MRI, [2]Neurosurgery, [3]Surgery, First Affiliated Hospital of Zhengzhou University, Zhengzhou, Henan

Received December 15, 2014; Accepted February 9, 2015; Epub March 15, 2015; Published March 30, 2015

Abstract: Cranial Mesenchymal chondrosarcoma (MC) and those that occurred in brain parenchymal were fairly rare aggressive neoplasm commonly affecting the bone of young adults. Here, we reported a case with intracranial MC, invading Broca's area, a rare site not previously reported, which was presumed to be a glioma. We performed a gross total resection guided by intra-operative magnetic resonance imaging (iMRI) combined with neuronavigation. Follow-up shows no language and other brain function loss. Furthermore, we present a review of literature. We emphasized the importance of gross total resection guiding by the combination of iMRI and neuronavigation, which was proved to be both reliable and effective in language preservation.

Keywords: Intracranial mesenchymal chondrosarcoma, intraoperative magnetic resonance, neuronavigation

Introduction

Mesenchymal chondrosarcoma (MC) is a rare aggressive neoplasm commonly affecting the bone of young adults. Cranial MC and those that occurred in brain parenchymal were extremely rare, which were associated with worse outcomes due to their invasive biology and proximity to vital brain structures. Here, we present a case with intracranial MC in Broca's area, a rare site not previously reported, which was presumed to be a glioma. We performed a gross total resection guided by intra-operative magnetic resonance imaging (iMRI) combined with neuronavigation. Follow-up showed no language and other brain function loss. Furthermore, we present a review of literature.

Case report

A 22-year-old female with a history of intermittent unclear speech (with no obvious incentives) and spontaneous remission after a few minutes. She was right-hand dominant. The medical history and routine laboratory studies were non-contributory. A magnetic resonance imaging (MRI) scan showed a well-demarcated mass measuring 18 × 15 × 17 mm in the left inferior frontal gyrus. The signal intensity of the lesion was higher than the grey matter on T1-weighted images and slightly higher than the grey matter on T2-weighted images (**Figure 1A**, **1B**). The peritumoral brain edema (PTBE) area had a higher signal intensity than the grey matter on fluid-attenuated inversion-recovery (FLAIR) images (**Figure 1C**). The lesion edge demonstrated ring-restricted diffusion with diffusion weighted imaging (DWI) (**Figure 1D**) and obvious enhancement with contrast was noted (**Figure 1E**). With magnetic resonance spectroscopic (MRS) imaging, the ratio of choline (Cho) to N-acetyl aspartate (NAA) in the tumor solid area was 3.12 (**Figure 1F**). On magnetic resonance perfusion imaging (PWI), the solid tumor area had high perfusion (**Figure 1G**). A glioma in the left inferior frontal gyrus was pre-operatively diagnosed.

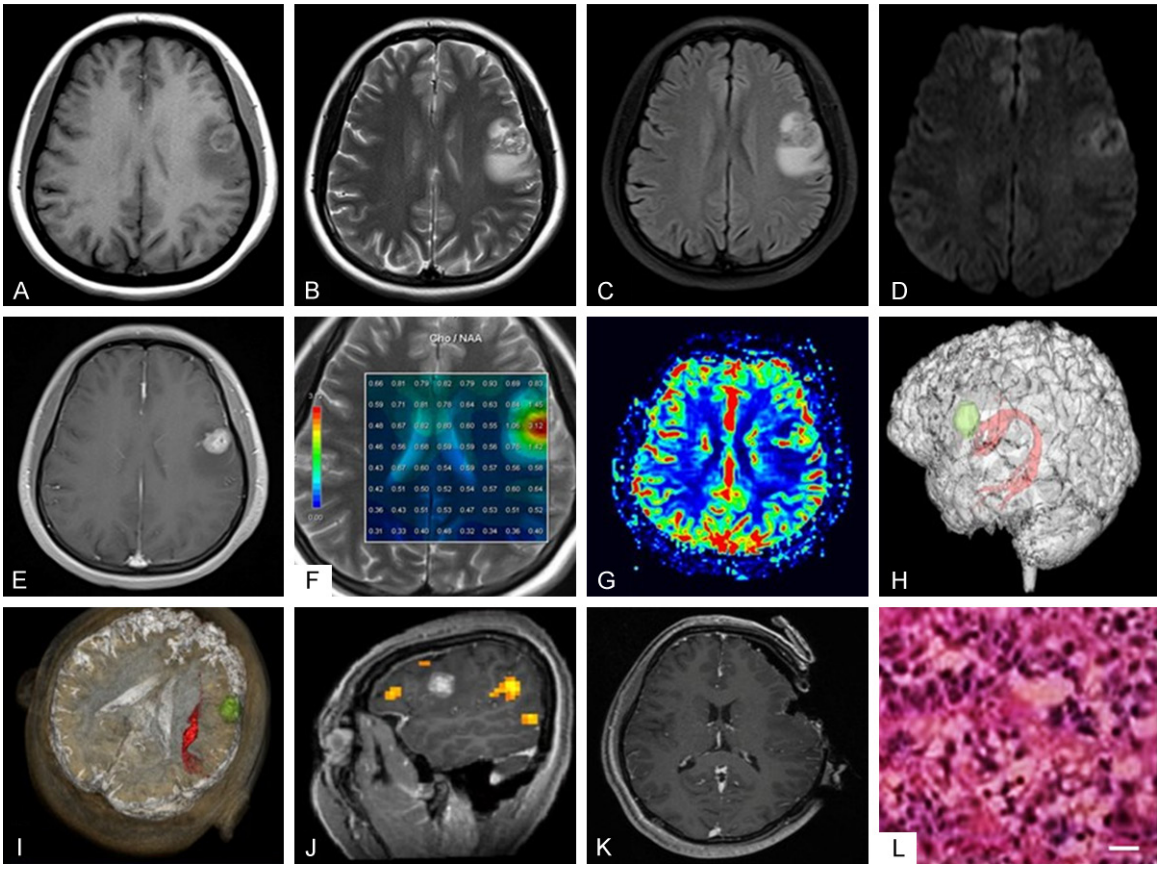

Figure 1. A. T1-weighted image showed that the signal intensity of the lesion was higher than the grey matter. B. T1-weighted image showed that the signal intensity of the lesion was slightly higher than the grey matter. C. Fluid-attenuated inversion-recovery (FLAIR) image showed that the PTBE area had a higher signal intensity than the grey matter. D. Diffusion weighted imaging (DWI) demonstrated ring-restricted diffusion around the lesion edge. E. MRI revealed an obvious enhancing lesion in the left inferior frontal gyrus. F. With MRS imaging, the ratio of Cho to NAA in the tumor solid area was 3.12. G. On PWI, the solid tumor area had high perfusion. H, I. The 3D reconstruction images disclose the relationship between the lesion and AF. J, The functional connectivity map demonstrated the relationship between the lesion and language areas. K. The intraoperative image indicated that there was no residual tumor. L. Photomicrograph of tumor specimen showed it is comprised of small, undifferentiated oval-to-spindle shaped cells. HE staining, scar bar ~20 μm.

Language function and cognitive state evaluation

Pre-operatively, language function was assessed by the Aphasia Battery of Chinese (ABC), which is the Chinese standardized adaptation of the Western Aphasia Battery. The Aphasia Quotient (AQ) score (spontaneous speech, comprehension, repetition and naming) was used to measure the language ability and the score was 100. The patient's pre-operative cognitive state was assessed by the Mini Mental State Examination (MMSE), and the score was 29.

Pre-operative examination and data processing

Pre-operative brain images were obtained in the diagnostic room of an iMRI-integrated neurosurgical suite (IMRIS, Winnipeg, Manitoba, Canada) using a movable 3.0-T scanner (MAGNETOM Verio 3.0T, Siemens AG, Erlangen, Germany) 1 day prior to the surgical intervention. The imaging protocol included a plain and contrast-enhanced three-dimensional (3D), magnetization-prepared, rapid-gradient echo (MPRAGE) sequence (time of repetition (TR), 1900 milliseconds; time of echo (TE), 2.93 milliseconds; flip angle, 9 degrees; matrix size, 256 × 215; slice thickness, 1 mm); diffusion tensor imaging (TR, 9900 milliseconds; TE, 90 milliseconds; slice thickness, 2 mm; slice space, 0 mm; matrix size, 128 × 128; voxel size, 2.0 × 2.0 × 2.0 mm^3; 30 directions); and resting-state blood oxygen level-dependent (BOLD) fMRI (TR, 2000 milliseconds; TE, 35 milliseconds; slice thickness, 4 mm; matrix size, 64 ×

64; voxel size, 3.3 × 3.3 × 4.0 mm^3; 240 time points) for the pre-operative identification of the language areas.

The arcuate fasciculus (AF) was reconstructed into a 3D object and was super-imposed onto the structural data using a post-processing workstation (Syngo MultiModality Workplace, Siemens AG). The reconstructed AF was defined with a two regions of interest (ROI) approach, as reported by Catani et al [1]. A fractional anisotropy (FA) threshold of 0.2, step length of 1mm, and angular threshold of 30° were used for AF tractography.

All resting-state fMRI data were pre-processed using Statistical Parametric Mapping 8 (SPM8; Welcome Department of Imaging Neuroscience, University College London, UK) and Data Processing Assistant for Resting-State fMRI-advanced edition (DPARSFA; by Yan and Zang, State Key Laboratory of Cognitive Neuroscience and Learning, Beijing Normal University, China) [2]. Standard image pre-processing was performed as follows. The first 10 volumes were discarded. The images were realigned and corrected for slice timing. The T1-weighted structural image was normalized to a Montreal Neurological Institute (MNI) template. The normalization parameters including the bounding box and voxel sizes, determining factors for the structural volume, were then applied to the functional image volume. A smoothing program with a Gaussian kernel of 4 mm was applied to the data. Linear trend over the run was removed. A temporal band-pass filter (0.01 Hz < f < 0.08 Hz) to the time course was used to obtain low-frequency fluctuations. Spurious BOLD variances that were unlikely to reflect neuronal activity were reduced, including signals from the cerebrospinal fluids, from the white matter and from the whole brain, as well as the six parameters obtained by rigid body head motion were correct. The BOLD fMRI time course was extracted from spherical seed ROI (3-mm radius) and then the seed-based functional connectivity map was generated. We created the seed ROI at the mirror region of Broca's area in the right hemisphere, and the coordinate of the seed ROI in the MNI space was at x = 47.45, y = 12.50 and z = 26.57 [3]. Then, we wrote the normalized functional images back to the patient's individual space. We used xjView 8 (http://www.alivelearn.net/xjview) to visualize the correlation map on the platform of Matlab. The threshold was determined according to the qualitative evaluation, which showed functional neuronal activity best while minimizing spatially non-specific noise that was probably of non-neuronal origin. In this patient, the functional connectivity map showed that the language areas located at the inferior frontal gyrus, angular gyrus and middle temporal gyrus.

The reconstructed series were imported into the surgical neuronavigation system. The relationships between the lesion, AF (**Figure 1H**, **1I**), and language areas (**Figure 1J**) were provided to the neurosurgeons for surgical planning.

Intraoperative MRI combined with neuronavigation-guided resection

On the day of surgery, the pre-operative plan and neuronavigation were combined, and the navigation was registered. Based on the surface projection of the tumor, the surgeons designed the operative incision and chose the best operative path. A conventional craniotomy was performed, and the brain surface was exposed. Then, the language areas were marked. By means of neuronavigation, the AF outlines could be displayed in the microscope field of view through the microscope heads-up display along with the tumor contour. The intraoperative visualization of the AF and marked language areas facilitated the preservation of the surrounding eloquent structures and maximized the tumor resection. Gross examination revealed that tumor was embedded in cerebrum and well-demarcated. The tumor tissue was well vascularized, grayish-white in color, and quite firm. The tumor was located in the left inferior frontal gyrus near the sylvian fissure with no evidence of dural attachment. When the surgeons confirmed the total removal of the tumor in the microscope, iMRI data were used to update the navigation information with the pre-operatively chosen method. The intraoperative images indicated that there was no residual tumor (**Figure 1K**). Tumor was total resected with less bleeding, the surgical time is 148 min. Only 50 ml blood was lost during total procedure. The update allowed the neurosurgeon to further resect the PTBE area, where the ratio of Cho to NAA was increased significantly in the pre-operative MRS image. Histologically, it was predominantly comprised of small, mostly

undifferentiated oval-to-spindle shaped cells. The cartilaginous component was variable, but was usually a minority of the tumor. The undifferentiated mesenchymal cells with rounded hyperchromatic nuclei and scant cytoplasm were arranged in better pattern around thin walled blood vessels. MC was pathologically diagnosed (**Figure 1L**).

Post-operative follow-up

One day after surgery, the patient spoke normally. Two days after surgery, the patient presented slurred speech. Three days after surgery, the patient presented complete aphasia, and five days after surgery, the patient began to improve. The same neuropsychologist performed the post-operative language function and cognitive state assessments. One week after surgery, the AQ score was 95.2 and the MMSE score was 27. One month after surgery, the patient's language function and cognitive state had recovered to the pre-operative level. The AQ score was 100, and the MMSE score was 29.

Discussion

Intracranial chondrosarcoma is an extremely rare intracranial tumor, accounting for 0.15% of all intracranial neoplasm [4]. MC is a less common subtype of chondrosarcoma first described by Lightenstein and Bernstein in 1959 [5]. Extraskeletal intracranial MCs mainly occur in the younger age (10~30 years), with a slight female preponderance [6]. MC was assumed to originate from the embryonal cartilaginous cells which rests in the cranial bones and dura, or from the meningeal fibroblasts, or from the multi-potent mesenchymal cells in the dura, arachnoid, or brain [7, 8]. Others believe that these cells are present in the arachnoid extensions that enclose the cerebral blood vessels. Yet other authors indicated that MC was the neoplasm of differentiating pre-mesenchymal chondroprogenitor cells, which are not restricted to bone but found throughout the body. The present tumor may have originated from multipotent mesenchymal or pre-mesenchymal chondroprogenitor cells in the brain parenchyma with no evidence of dural attachment. A whole body survey was performed in the present patient, and no extracranial lesions were identified. Intracranial MC is more aggressive, with a very high frequency of local recurrence and distant metastasis. The overall 5- and 10-year survival of patients with MC, when considering all sites, is 55% and 27%, respectively [9]. The treatment strategy is the radical removal of these lesions, regardless of the anatomical site [4, 6, 9-11]. A partial tumor resection accelerates recurrence, and repeated surgeries promote invasion and metastasis. Furthermore, resection adjacent to the eloquent area poses a great challenge of maximizing tumor removal and protecting language function. The protection of language function during surgery not only requires the preservation of the language cortex but also the location and protection of subcortical language tracts [12]. Intraoperative electrostimulation is considered as the gold standard for functional localization [13]. However, it is an invasive procedure that have to awake patients, and it is also hard to make pre-operative planning and clarify post-operative language function recovery mechanisms. In this report, we solved this problem through the combination of iMRI and neuronavigation.

According to the current literatures [4, 6, 9-11] neuronavigation-guided resection of intracranial MCs under general anesthesia should be the first choice. There is currently no detailed information on how to maximize MC resection while preserving the surrounding eloquent structures.

The present intracranial MC was located in the left inferior frontal gyrus, which is an important language area (Broca's area). In this study, we generated fiber tract images of the AF and language cortex from functional neuroimaging, including DTI and resting-state fMRI data. Combined with neuronavigation, the imaging enabled the neurosurgeon to accurately define the tumor outline, language cortex, AF, and their relationships. All these were helpful to choose the best approach. Following the opening of the dura, the neurosurgeon marked the language cortex. The AF outlines could be displayed in the microscope field of view through the microscope heads-up display along with the tumor contour. By means of neuronavigation, the contour display in the surgical field could provide a very intuitive 3D impression of the AF course and tumor, allowing the surgeon to maximize tumor resection without damaging the surrounding areas. A second iMRI scan revealed that total tumor excision was achieved. Our

patient experienced no language function and cognitive state deficits for one month after surgery. The MRI images demonstrated the integrity of the language cortex and AF. This result indicated that the intraoperative identification and location of structural and functional nerve tissues were essential for the protection of neurological function.

Spontaneous BOLD fluctuations were identified by Biswal and Fox in 1995, applying seed-based functional connectivity to analyze the resting-state fMRI data [14]. Further research confirmed that functional connectivity existed in the motor, auditory, visual, and language systems, which reflected brain activity during the resting state [3, 15]. The brain functional imaging techniques of DTI were developed based on DWI. By measuring the water diffusion in different planes and tracing the pathway of least hindrance to diffusion, DTI tractography can reveal continuous neural pathways based on the movement of water molecules subjected to a magnetic gradient. Resting-state fMRI and DTI-based fiber tracking technology are widely applied to pre-operatively identify the location of the language cortex and subcortical language pathways in brain tumor patients, which is coincident with intraoperative electrostimulation [16]. Through resting-state fMRI and DTI technology, the major functional areas, including Broca's and Wernicke's areas and AF, can be reconstructed. In combination with a neuronavigation system, the anatomical relationship between the tumor and eloquent structures relevant to language can be visualized, allowing the operator to remove a lesion as precisely as possible while preserving primary functions. High-field iMRI yields high-quality intraoperative brain anatomical images and functional imaging. Functional imaging, including DTI and resting-state fMRI, can be used for an immediate update of the shifted structures relevant to language in relation to the resection cavity or residual tumor. The update allows the surgeon to correct for brain shifts with conventional neuronavigation. IMRI combined with neuronavigation facilitates tumor removal while preserving the integrity of neurological function. Thus, the disability rate is decreased, and the quality of life is improved.

PTBE is a common incidental sign of a tumor, which is related to the presence or growth of the tumor. PTBE is the basis of invasion and metastasis of tumor cells within the normal brain tissue. However, the invasion and metastasis of tumor cells in the PTBE area cannot be identified via abnormal changes in morphology and are not detected with conventional MRI, which complicates the surgical planning and identification of the tumor margin. As a minimally invasive examination method, MRS, which utilizes the magnetic resonance phenomena and chemical shifts, can specifically analyze the atomic nucleus and their compounds and provide information on brain metabolism and biochemistry. N-acetyl aspartate (NAA), which only exists in nerve tissues, is a sign of neuronal degeneration and death, and choline (Cho) is a sign of tumor cell proliferation [17]. Ricci et al. found that the PTBE had a pathological spectrum of increased Cho levels and reduced NAA levels, which might be relevant to tumor cell invasion [18]. Intracranial MC is more aggressive, with a very high frequency of local recurrence and distant metastasis. Therefore, removing potential tumor cells in the PTBE area as extensively as possible is an important approach to prevent recurrence. Thus, the pathological examination was performed in the PTBE area where potential tumor cells resided, i.e., where the ratio of Cho to NAA was significantly increased in this study. The result indicated that there was no tumor cell invasion.

Conclusion

Here, we reported a case with intracranial MC, invading Broca's area. We emphasized the importance of gross total resection guiding by the combination of iMRI and neuronavigation, which was proved to be both reliable and effective in language preservation.

Acknowledgements

This study was supported by the Henan Province Health Department (201303044).

Disclosure of conflict of interest

None.

Address correspondence to: Bo Yang, Department of Neurosurgery, First Affiliated Hospital of Zhengzhou University, No. 1, Road Jiangshe, District Erqi, Zhengzhou 450052, Henan, China. E-mail: Yang_BoBY@163.com

References

[1] Catani M, Howard RJ, Pajevic S, Jones DK. Virtual in vivo interactive dissection of white matter fasciculi in the human brain. Neuroimage 2002; 17: 77-94.

[2] Chao-Gan Y, Yu-Feng Z. DPARSF: A MATLAB Toolbox for "Pipeline" Data Analysis of Resting-State fMRI. Front Syst Neurosci 2010; 4: 13.

[3] Raichle ME. The restless brain. Brain Connect 2011; 1: 3-12.

[4] Bloch OG, Jian BJ, Yang I, Han SJ, Aranda D, Ahn BJ, Parsa AT. A systematic review of intracranial chondrosarcoma and survival. J Clin Neurosci 2009; 16: 1547-1551.

[5] Lightenstein L, Bernstein D. Unusual benign and malignant chondroid tumors of bone. a survey of some mesenchymal cartilage tumors and malignant chondroblastic tumors, including a few multicentric ones, as well as many atypical benign chondroblastomas and chondromyxoid fibromas. Cancer 1959; 12: 1142-1157.

[6] Vergeer RA, Vink R, Avenarius JK, Driesse MJ. A 71-year-old woman with an intracranial dural-based mesenchymal chondrosarcoma. J Clin Neurosci 2012; 19: 1170-1171.

[7] Harsh GR 4th, Wilson CB. Central nervous system mesenchymal chondrosarcoma. Case report. J Neurosurg 1984; 61: 375-381.

[8] Steiner GC, Mirra JM, Bullough PG. Mesenchymal chondrosarcoma. a study of the ultrastructure. Cancer 1973; 32: 926-939.

[9] Kan Z, Li H, Zhang J, You C. Intracranial mesenchyma chondrosarcoma: case report and literature review. Br J Neurosurg 2012; 26: 912-914.

[10] Vij M, Krishnani N, Agrawal V, Jaiswal S, Kumari N, Jaiswal AK, Behari S. Cytomorphology of intraparenchymal mesenchymal chondrosarcoma in frontal lobe: report of a case. Diagn Cytopathol 2011; 39: 837-842.

[11] Little A, Chung C, Perez-Ordonez B, Mikulis D, Valiante TA. High-grade intracranial chondrosarcoma presenting with haemorrhage. J Clin Neurosci 2013; 20: 1457-1460.

[12] Wu JS, Zhang J, Zhuang DX, Yao CJ, Qiu TM, Lu JF, Zhu FP, Mao Y, Zhou LF. Current status of cerebral glioma surgery in China. Chin Med J (Engl) 2011; 124: 2569-2577.

[13] Lu J, Wu J, Yao C, Zhuang D, Qiu T, Hu X, Zhang J, Gong X, Liang W, Mao Y, Zhou L. Awake language mapping and 3-Tesla intraoperative MRI-guided volumetric resection for gliomas in language areas. J Clin Neurosci 2013; 20: 1280-1287.

[14] Biswal B, Yetkin FZ, Haughton VM, Hyde JS. Functional connectivity in the motor cortex of resting human brain using echo-planar MRI. Magn Reson Med 1995; 34: 537-541.

[15] Raichle ME. A brief history of human brain mapping. Trends Neurosci 2009; 32: 118-126.

[16] Leclercq D, Duffau H, Delmaire C, Capelle L, Gatignol P, Ducros M, Chiras J, Lehéricy S. Comparison of diffusion tensor imaging tractography of language tracts and intraoperative subcortical stimulations. J Neurosurg 2010; 112: 503-511.

[17] Sibtain NA, Howe FA Saunders DE. The clinical value of proton magnetic resonance spectroscopy in adult brain tumours. Clin Radiol 2007; 62: 109-119.

[18] Ricci R, Bacci A, Tugnoli V, Battaglia S, Maffei M, Agati R, Leonardi M. Metabolic findings on 3T 1H-MR spectroscopy in peritumoral brain edema. AJNR Am J Neuroradiol 2007; 28: 1287-1291.